Earth and Planetary Science Letters 403 (2014) 27–36

Contents lists available at ScienceDirect

Earth and Planetary Science Letters

www.elsevier.com/locate/epsl

Geological respiration of a mountain belt revealed by the trace element rhenium

Robert G. Hilton [a,b,*], Jérôme Gaillardet [b], Damien Calmels [c,d], Jean-Louis Birck [b]

[a] Department of Geography, Durham University, Science Laboratories, South Road, Durham, DH1 3LE, UK
[b] Equipe de Géochimie et Cosmochimie, Institut de Physique du Globe de Paris, Sorbonne Paris Cité, Univ Paris Diderot, UMR 7154 CNRS, F-75005 Paris, France
[c] Equipe de Géochimie des Isotopes Stables, Institut de Physique du Globe de Paris, Sorbonne Paris Cité, Univ Paris Diderot, UMR 7154 CNRS, F-75005 Paris, France
[d] Department of Earth Sciences, University of Cambridge, Cambridge, CB2 3EQ, UK

ARTICLE INFO

Article history:
Received 7 January 2014
Received in revised form 9 June 2014
Accepted 12 June 2014
Available online xxxx
Editor: T.M. Harrison

Keywords:
carbon cycle
organic carbon
rhenium
weathering
erosion
mountain rivers

ABSTRACT

Oxidation of rock-derived, petrogenic, organic carbon (OC_{petro}) during weathering of sedimentary rocks is a major source of carbon dioxide (CO_2) to the atmosphere. This geological respiration is thought to be enhanced by physical erosion, suggesting that mountain belts could release large amounts of CO_2 to counter the CO_2 sequestration achieved by the erosion, riverine transfer and oceanic burial of organic carbon from the terrestrial biosphere. However, OC_{petro} oxidation rates in mountain belts have not been quantified. Here we use rhenium (Re) as a proxy to track OC_{petro} oxidation in mountain river catchments of Taiwan, where existing measurements of physical erosion rate allow the controls on OC_{petro} oxidation to be assessed. Re has been shown to be closely associated with OC_{petro} in rocks and following oxidation during chemical weathering forms a soluble oxyanion (ReO_4^-) which contributes to the dissolved load of rivers. Soils on meta-sedimentary rocks in Taiwan show that Re loss is coupled to OC_{petro} loss during weathering, confirming previous observations from soil profiles on sedimentary rocks elsewhere. In Taiwan rivers, dissolved Re flux increases with the catchment-average sediment yield, suggesting that physical erosion rate is a major control on OC_{petro} oxidation. Based on our current understanding of Re mobility during weathering, the dissolved Re flux can be used to quantify an upper bound on the OC_{petro} oxidation rate and the associated CO_2 transfer. The estimated CO_2 release from this mountain belt by OC_{petro} oxidation does not negate estimates of CO_2 sequestration by burial of biospheric OC offshore. The findings are compared to OC transfers estimated for the Himalaya, where OC_{petro} oxidation in the mountain belt remains unconstrained. Together, these cases suggest that mountain building in the tropics can result in a net sink of OC which sequesters atmospheric CO_2.

1. Introduction

Organic matter within sedimentary rocks constitutes a vast stock of carbon that was sequestered from the atmosphere in the geological past, containing $\sim 15 \times 10^{15}$ gC which is ~25 000 times the carbon content of the pre-industrial atmosphere (Sundquist and Visser, 2005). Oxidation of this rock-derived, or 'petrogenic', organic carbon (OC_{petro}) during weathering at Earth's surface is a major source of CO_2 to the atmosphere and sink of O_2 (Berner and Canfield, 1989; Derry and France-Lanord, 1996). Better understanding the balance between OC_{petro} oxidation and the sedimentary burial of recently photosynthesized organic carbon from the terrestrial biosphere ($OC_{biosphere}$) is fundamental to assessing how atmospheric CO_2 and O_2 concentrations have evolved over geological time (Hayes et al., 1999; Hayes and Waldbauer, 2006). OC_{petro} oxidation is thought to occur when sedimentary rocks are exposed to aqueous and gas phase O_2 (Chang and Berner, 1999), with the rate of CO_2 release controlled by the supply of OC_{petro} to react (Petsch et al., 2000; Bolton et al., 2006). As such, mountain belts where high rates of physical erosion can supply abundant OC_{petro} to the surface (Galy et al., 2008a; Hilton et al., 2011) may be locations where this CO_2 source is most potent. If true, OC_{petro} oxidation may counter the CO_2 consumption achieved by the erosion of $OC_{biosphere}$ and its efficient preservation and burial in sedimentary deposits of these settings (France-Lanord and Derry, 1997; Stallard, 1998; Galy et al., 2007; Kao et al., 2014). In order to assess the net impact of mountain building on CO_2 fluxes to and from the atmosphere (Caldeira et al., 1993; Derry and France-Lanord, 1996; Gaillardet and Galy, 2008), the rates of OC_{petro} oxidation during weathering in mountain belts must be quantified.

* Corresponding author at: Department of Geography, Durham University, Science Laboratories, South Road, Durham, DH1 3LE, UK. Tel.: +44 0191 33 41970.
E-mail address: r.g.hilton@durham.ac.uk (R.G. Hilton).

http://dx.doi.org/10.1016/j.epsl.2014.06.021

OC_{petro} oxidation has been shown to be significant during the floodplain transport of clastic sediments eroded from the Himalaya and Andes mountain ranges in the Ganges and Amazon rivers, respectively (Galy et al., 2008a; Bouchez et al., 2010). However the method employed, which used the radiocarbon content of OC in river suspended load to determine OC_{petro} loss from the solid phase, did not have the resolution necessary to quantify OC_{petro} oxidation rate in the mountain catchments where it should be most rapid. This is because chemical denudation rates are usually ~0.01–0.1 times lower than physical denudation rates in mountain belts (Jacobson and Blum, 2003; West et al., 2005), so suspended sediments in mountain rivers have a geochemical composition similar to bedrocks (Hilton et al., 2010). Therefore it is difficult to use the solid products of weathering carried by rivers to quantify OC_{petro} oxidation in mountain catchments (Hilton et al., 2011). An alternative approach is to track the products of chemical weathering carried in the dissolved load of rivers (Meybeck, 1987; Gaillardet et al., 1999) which has provided detailed constraints on chemical weathering processes and inorganic carbon fluxes from mountain catchments (Jacobson and Blum, 2003; West et al., 2005; Calmels et al., 2011).

The trace element rhenium (Re) is a strong candidate to act as a proxy for OC_{petro} oxidation during weathering as suggested by previous work (Dalai et al., 2002; Jaffe et al., 2002) due to: i) its association with OC_{petro} in rocks; and ii) its redox-dependent solubility, factors which are closely linked. In oxygenated waters (Eh > 0 V), Re is dominantly present as the soluble perrhenate oxyanion (ReO_4^-) over a wide range of pH values (5.5 to 9.5) (Brookins, 1986) and in seawater Re behaves conservatively (Anbar et al., 1992; Colodner et al., 1993). In marine depositional environments, OC-bearing sediments experience reduction of ReO_4^- contained in seawater and Re forms a solid phase (Colodner et al., 1993; Crusius et al., 1996; Crusius and Thomson, 2000). Isolation of organic matter from marine sedimentary rocks has suggested that Re is complexed to OC_{petro} in the depositional environment, favoring organic chelating sites to co-existing sulfide phases, both in marine sediments with high organic contents (Cohen et al., 1999; Selby and Creaser, 2003) and relatively organic-poor sediments (Pierson-Wickmann et al., 2002; Rooney et al., 2012).

When these sedimentary rocks are re-exposed, for example by erosion and exhumation during orogenesis (e.g. Hilton et al., 2011), Re-bearing OC_{petro} is subject to chemical weathering in oxic surface environments (Petsch et al., 2000; Jaffe et al., 2002; Pierson-Wickmann et al., 2002). Previous weathering studies from soils on OC-rich rocks have demonstrated that Re loss tracks the OC_{petro} loss (Jaffe et al., 2002). In contrast, oxidative weathering of sulfide minerals continued much deeper into the soil profile where OC_{petro} and Re were still found at concentrations similar to the unweathered bedrock (Jaffe et al., 2002). While the fate of gaseous CO_2 released by OC_{petro} oxidation is difficult to trace at the catchment scale (Keller and Bacon, 1998), Re will be oxidized to the soluble ReO_4^- (Brookins, 1986). Re is not thought to be cycled through the modern terrestrial biosphere (cf. to molybdenum which is used in nitrogenase), meaning that the mobilized ReO_4^- enters the hydrological network (Brookins, 1986; Colodner et al., 1993; Miller et al., 2011). Rivers integrate chemical reactions and hydrological sources across the landscape (Gaillardet et al., 1999), thus the dissolved Re flux can be interpreted as the result of oxidative weathering reactions occurring upstream (Dalai et al., 2002). Building on previous work, which has established the close affinity of Re and OC_{petro} in sedimentary rocks and their coupled behavior during oxidative weathering, OC_{petro} oxidation rates may be quantified from the dissolved Re flux, provided the Re to OC_{petro} ratio of the rocks which have undergone weathering is known.

Here we examine the transfer of Re in mountain rivers with high erosion rates with a view to assessing the controls on OC_{petro} oxidation, while estimating the associated CO_2 release across a mountain belt for the first time. We focus on major rivers in Taiwan, where river gauging records constrain the rates and patterns of physical erosion (Dadson et al., 2003) and previous work has quantified the erosion of $OC_{biosphere}$ (Hilton et al., 2012) and tracked its preservation in marine sediments offshore (Kao et al., 2014). For the first time, this allows the role of erosion on OC_{petro} oxidation to be assessed, and means that an OC budget is within reach for the mountain belt. We examine the mobility of Re from the solid phase during chemical weathering in soils from Taiwan, and measure the dissolved Re concentration in the major rivers. We discuss in detail the assumptions required to use Re as a quantitative proxy of OC_{petro} oxidation, in light of the new data from Taiwanese soils and previous work on Re mobility during weathering. Our estimates of dissolved Re flux provide new insight on the major controls on OC_{petro} oxidation and provide an upper bound estimate of the associated CO_2 release, allowing us to better assess the impact of orogenesis on the carbon cycle.

2. Materials and methods

2.1. Setting

Taiwan formed by the collision of the Luzon Arc on the Philippine Sea Plate with the Eurasian continental margin. Rapid tectonic uplift and seismicity combine with a tropical cyclone climate to drive high physical erosion rates, coupling river incision and bedrock landsliding on steep slopes (Hovius et al., 2000). Suspended sediment yields have been quantified from 1970 for the major rivers and vary around the island, reaching amongst the highest in the world at $>10\,000\ t\,km^{-2}\,yr^{-1}$ (Dadson et al., 2003). Rapid physical erosion and turnover of the landscape by landslides results in thin soils (<0.8 m) (Tsai et al., 2001) and high rates of erosion and fluvial export of $OC_{biosphere}$ (Hilton et al., 2012) which is exported to the ocean and preserved efficiently in marine sediments (Kao et al., 2014).

Exhumation in the Central Range has exposed passive margin sedimentary rocks which contain ~0.2–0.4 weight% OC_{petro} (Hilton et al., 2010). Peak metamorphic temperatures decrease from east (~500 °C) to west (<150 °C) across the range (Beyssac et al., 2007). Raman Spectroscopy reveals that OC_{petro} can be present as graphite in the Tananao Schist and Pilushan formations (Fig. S1) in the eastern flank of the Central Range mountains (Beyssac et al., 2007). Deep-seated bedrock landslides can mobilize unweathered OC_{petro} along with surface soils and contribute OC_{petro} to the suspended load of Taiwanese rivers (Hilton et al., 2010), as in other mountain river systems (Clark et al., 2013). Once in the fluvial network, the suspended sediment and OC_{petro} is rapidly exported with minimal time for subsequent oxidation (Hilton et al., 2008a, 2011). As a result, the solid load of mountain rivers in Taiwan is dominated by unweathered erosion products (Selvaraj and Chen, 2006) and Taiwan delivers ~1.7 $MtC\,yr^{-1}$ of OC_{petro} to the ocean in solid form (Hilton et al., 2011).

2.2. Samples

River water samples were collected for this study and combined with existing samples of river water (Calmels et al., 2011), river bed materials (Hilton et al., 2010) and soils (Hilton et al., 2013). River waters for this study were collected from major rivers in Taiwan during the typhoon season in September 2007 following several days rainfall (Table S1). To establish the hydrological controls on Re transfer, four additional samples were analyzed from a suite collected in 2004 (Calmels et al., 2011) during a typhoon flood when daily runoff (water discharge normalized by the upstream area, $mm\,day^{-1}$) reached >10 times

the long-term mean. Surface waters from turbulent rivers were collected using established methods for Re (Dalai et al., 2002; Miller et al., 2011) in thoroughly rinsed LDPE bottles and filtered immediately through 0.2 μm nylon filters into acid-cleaned trace analysis grade Nalgene LDPE bottles rinsed with filtered river water, then acidified to pH ~ 2 (trace analysis grade HNO_3). An additional un-acidified aliquot was collected for major anions. Filtered samples were stored at 4 °C in the dark. Daily water discharge (m^3/s) was obtained from the Water Resources Agency, Taiwan.

To assess the geochemical composition of rocks at the scale of river catchments (e.g. Tipper et al., 2006; Galy et al., 2008b) river bed materials previously collected from three major river catchments (Hilton et al., 2010) were analyzed. These drain a range of geological formations which are representative of the wider Central Range, Taiwan (Fig. S1; Table S2). As described by Hilton et al. (2010), ~500 cm^3 of sand material were collected from alluvium deposited in bedrock channels at low flow in March 2006. The majority of these sediments were deposited following the flood associated with Typhoon LongWang (October 2005) (Turowski et al., 2008) and were likely to have been sourced by 100–1000s of bedrock landslides upstream (Hovius et al., 2000). Given the transient nature of sediment storage in Taiwan rivers and the short fluvial transit times (Hilton et al., 2008a), these river bed materials can provide constraint on catchment-averaged bedrock composition.

To assess whether the coupled loss of Re and OC_{petro} observed elsewhere in OC-rich bedrocks occurs during weathering of rocks in Taiwan, solid weathering products collected from upper soil horizons in the Wulu catchment were used (Fig. S1). These were collected by Hilton et al. (2013), as ~500 cm^3 of soil over a depth of ~10 cm, corresponding to A and E Horizons of variable humified organic matter with coarse and fine fractions bearing little structure of existing bedrock. Prior to analysis, soil and river bed materials samples were each homogenized to an integrated bulk sample.

2.3. Rhenium concentration

Re concentrations in river waters ($[Re]_{diss}$) are typically low ($pmol\,L^{-1}$) and so an established anion-exchange column chemistry technique was used to pre-concentrate Re and remove the sample matrix (Huffman et al., 1956; Birck et al., 1997). In summary, 100 ml of sample was loaded onto 3 ml of AG1-X8 (200–400 mesh) resin at 0.1 N HNO_3 and eluted to cleaned Teflon at 4 N HNO_3. Re recovery was quantified using standard solutions (Re-filament dissolved in HNO_3) and matrix effects assessed by Re addition to river samples. Purified eluted residues were re-taken in 3% HNO_3 and analyzed by quadrupole inductively-coupled-plasma mass spectrometry (Q-ICP-MS). The full procedural blank was 1.8 pg, ~2% of the typical sample mass of Re, similar to published methods (Dalai et al., 2002). Standards with similar concentrations as samples not used to construct calibration curves had average precision of 3%. Sample reproducibility was 5% which is taken as the precision on the analyses. Recovery during column chemistry was 100% within this precision. To analyze smaller volume water samples (<20 ml) we developed a standard-addition (SA) method for which pre-concentration is not required and the use of HNO_3 is minimized, the major blank contributor (Birck et al., 1997). A set of samples analyzed by Q-ICP-MS following anion-exchange chemistry were also analyzed by SA, using a minimum of three additions, with strong agreement between the measurements across the dataset ($y = 0.96 \pm 0.02x$, $r = 0.99$, $P < 0.0001$) suggesting $[Re]_{diss}$ by SA-Q-ICP-MS is precise to better than 10% in these samples.

In solid samples, [Re] was determined by isotope dilution following established methods (Birck et al., 1997). 50 mg of powder was weighed to Teflon bombs and a ^{185}Re enriched-spike was added to each sample. Following equilibration, digestion was achieved with 4 ml of concentrated distilled HF:HNO_3 at 150 °C. Re was extracted using 3-methyl-1-butanol (iso-amylol) liquid–liquid extraction (Birck et al., 1997). The purified sample was re-taken in 3% HNO_3, analyzed by Q-ICP-MS and corrected for the procedural blank.

2.4. Major ion and elemental concentrations

In river water, major ion concentrations were analyzed by Ion Chromatography (Table S1). In river bed materials and soils, total sulfur concentrations were determined by combustion and major elements (CaO and Al_2O_3) determined by ICP-OES at SARM, CRPG, Nancy (Table S2). The OC and nitrogen concentrations (%) were measured in previous work following inorganic carbon removal (Hilton et al., 2010, 2013). The radiocarbon activity of soil samples was also determined by Hilton et al. (2013) and is reported here as the fraction modern (F_{mod}) corrected to $-25‰$ $\delta^{13}C_{VPDB}$ based on measured stable isotope composition, where $F_{mod} = 1$ is the ^{14}C content of 1950 atmosphere and $F_{mod} = 0$ is a sample which contains no measurable ^{14}C (Stuiver and Polach, 1977). The OC_{petro} content of soil samples was quantified using F_{mod} measurements and a binary mixing model as outlined in Appendix A.

3. Results

3.1. Dissolved rhenium in Taiwan rivers

In river waters, $[Re]_{diss}$ range from 4.7 ± 0.2 $pmol\,L^{-1}$ to 25.4 ± 1.2 $pmol\,L^{-1}$ (Table S1) which are toward the higher end of published data from global rivers (Fig. 1A) (Colodner et al., 1993; Dalai et al., 2002; Miller et al., 2011; Rahaman et al., 2012). Differences in $[Re]_{diss}$ between catchments in Taiwan (RSD = 53%) are greater than the mean variability of $[Re]_{diss}$ in a single river catchment (RSD < 22%). Some of this variability is linked to the runoff at the time of sampling, with $[Re]_{diss}$ positively correlated with runoff (Fig. 1B; $r = 0.65$, $P = 0.02$). However, samples collected from the Liwu River during a flood event have $[Re]_{diss}$ values which are relatively invariant (8% RSD) while runoff varied by up to >10 the long term mean (Fig. 1B). The findings are consistent with measurements from Arctic rivers, which did not show a significant relationship between water discharge and $[Re]_{diss}$ (Miller et al., 2011). This contrasts strongly with some major elements which tend to show dilution at high runoff (e.g. Tipper et al., 2006), such as [Na] which is strongly negatively correlated with runoff in the sample set (Fig. 1C; $r = -0.88$, $P = 0.004$) and during the flood event (Calmels et al., 2011). The dilution of [Na] is consistent with elements mobilized predominantly by acid hydrolysis reactions during silicate weathering (Calmels et al., 2011; Maher et al., 2011).

In the absence of a major hydrological control on $[Re]_{diss}$, we examined other controls on $[Re]_{diss}$. In contrast to previous work (Dalai et al., 2002; Miller et al., 2011), there was no significant correlation between $[SO_4]$ and $[Re]_{diss}$ in Taiwan (Fig. 1A; $P = 0.25$). $[Re]_{diss}$ was correlated with [K] ($r = 0.62$, $P = 0.008$), supporting recent findings from Indian rivers with minimal anthropogenic disturbance (Rahaman et al., 2012). In the flood event samples where the instantaneous suspended sediment concentration ($mg\,L^{-1}$) was measured ($n = 4$), there was no significant correlation with $[Re]_{diss}$ ($P = 0.07$). The most significant correlation with $[Re]_{diss}$ was with the catchment average suspended sediment concentration measured over 30 yr (Fig. 2; $r = 0.84$, $P < 0.0001$). This is a measure of decadal physical erosion rate normalized by catchment runoff (Dadson et al., 2003). In addition to this trend, catchments draining higher grade metamorphic rocks

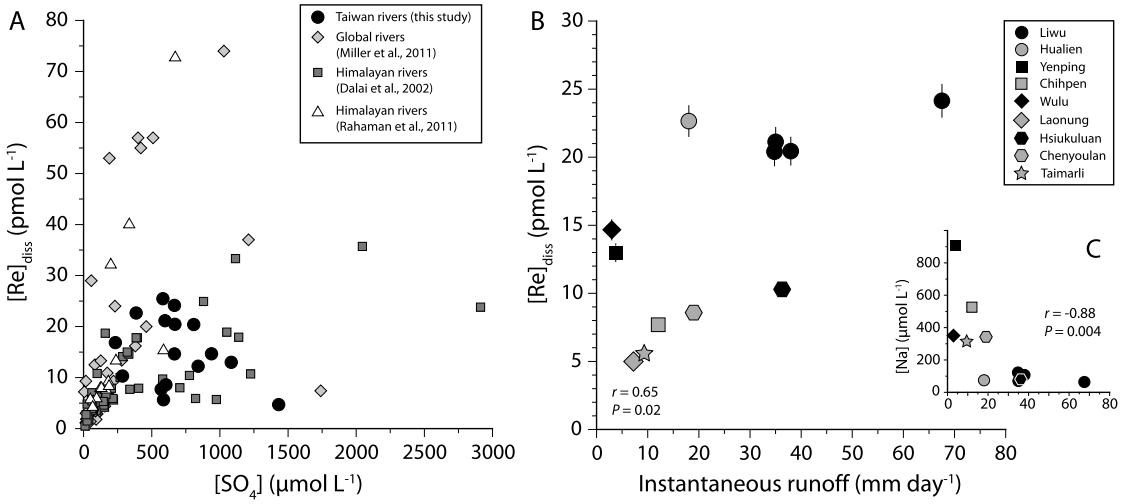

Fig. 1. A. Dissolved rhenium concentration, $[Re]_{diss}$ (pmol L^{-1}), versus sulfate concentration, $[SO_4]$ (μmol L^{-1}), for Taiwan rivers (black circles) and a global river compilation (Dalai et al., 2002; Miller et al., 2011; Rahaman et al., 2012). Across all measurements there is a positive correlation ($r = 0.44$; $P < 0.0001$) but considerable scatter, and values are not correlated for the Taiwan dataset ($P = 0.25$). **B.** $[Re]_{diss}$ versus instantaneous runoff (mm day^{-1}) for Taiwan river samples (labeled by catchment). **C.** Dissolved sodium concentration, [Na] (μmol L^{-1}), versus instantaneous runoff for the same samples shown in part B. Bars indicate the precision on the analysis where larger than the point size.

in the northeast flank of the Central Range (Beyssac et al., 2007; Hilton et al., 2010), such as the Liwu, Hualien, Hsiukuluan (Fig. S1), appear to have slightly higher $[Re]_{diss}$ than catchments draining lower grade metamorphic rocks at similar erosion rates (Laonung, Chihpen). However, the scatter in the relationship (Fig. 2) may also be controlled by hydrological variability in $[Re]_{diss}$ (Fig. 1B) and longer-term records of $[Re]_{diss}$ are needed to examine second order trends in detail.

3.2. Rhenium in river bed materials and soils

The river bed materials in Taiwan represent the solid products of erosion and have [Re] values which range from 0.60 to 0.96 ppb (Table S2). These are lower than measured in one of the first studies to propose Re as a tracer of OC_{petro} oxidation, with [Re] = 75–116 ppb in a Devonian black shale (Jaffe et al., 2002). The difference is mirrored by the low OC_{petro} content of river bed materials in Taiwan, $[OC_{petro}] = 0.17–0.23\%$, compared to $[OC_{petro}] = 6.0–7.8\%$ in the Devonian shale (Jaffe et al., 2002). However, [Re] in Taiwanese river bed sediments are similar to river bed sediments measured in the Himalaya of [Re] < 1.2 ppb (Rahaman et al., 2012) and Himalayan rocks (Pierson-Wickmann et al., 2002) where OC_{petro} contents of river bed loads are similar to Taiwan, with $[OC_{petro}] < 0.2\%$ (Galy et al., 2008b). The [Re] of river bed materials from Taiwan are also similar to modern marine sediments in sub-oxic waters (Crusius and Thomson, 2000), where OC contents and [Re] are lower than sediments in anoxic basins (Ravizza et al., 1991). We note that [Re] may vary with the grain size of river bed materials in analogy to major elements (Bouchez et al., 2011), however, a larger sample set is necessary to establish these controls.

The mean ratio of [Re] to $[OC_{petro}]$ in the three river bed material samples is 3.7×10^{-7} and the values range within a factor of two from 2.6×10^{-7} to 4.6×10^{-7}. These ratios are lower than those measured on two sets of OC-rich Devonian black shale, with mean $[Re]:[OC_{petro}] = 12.8 \pm 3.4 \times 10^{-7}$ ($n = 5$, ±2 SE) (Jaffe et al., 2002) and mean $[Re]:[OC_{petro}] = 12.2 \pm 5.0 \times 10^{-7}$ ($n = 8$, ±2 SE) (Selby and Creaser, 2003). However, they are similar to OC-rich Jurassic shale (mean $[OC_{petro}] = 20 \pm 8\%$) with mean $[Re]:[OC_{petro}] = 3.5 \pm 0.9 \times 10^{-7}$ ($n = 5$, ±2 SE) (Cohen et al., 1999). The differences in $[Re]:[OC_{petro}]$ between localities is expected given the different redox conditions, sedimentation rates and bioturbation

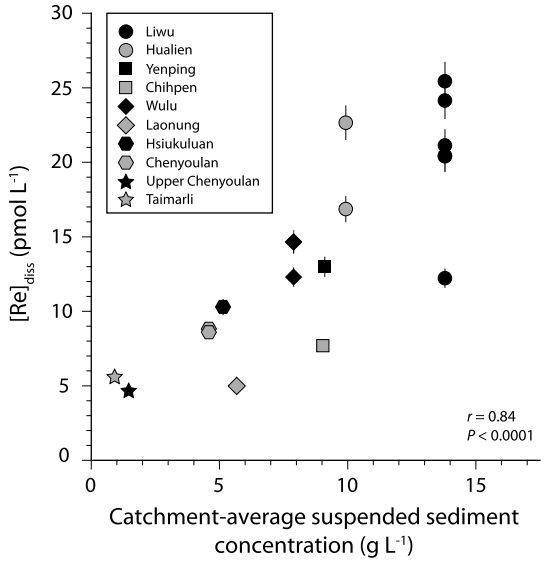

Fig. 2. Dissolved rhenium concentration ($[Re]_{diss}$ in pmol L^{-1}) for Taiwan rivers sampled in 2004 and 2007 versus the catchment average suspended sediment concentration for 1970–1999 (Dadson et al., 2003) (errors not provided) a measure of physical erosion per unit of water runoff. Vertical lines show analytical precision (if larger than the point size).

rates likely to have occurred at the time of burial, which will influence the [Re] and $[OC_{petro}]$ (McKay et al., 2007). In addition, the $[Re]:[OC_{petro}]$ may vary with metamorphic grade and the thermal maturity of OC_{petro}, although this remains poorly constrained (Rooney et al., 2012; Cumming et al., 2014). Nevertheless, the results confirm the importance of constraining a local $[Re]:[OC_{petro}]$ in upstream lithologies when using Re to examine OC_{petro} weathering (Dalai et al., 2002).

The thin surface soils have low $[OC_{petro}] < 0.05\%$ (Table S2), consistent with oxidative loss of OC_{petro} during weathering. The bulk soils have [Re] = 0.07–0.19 ppb, lower than the river bed materials. Soils are also depleted in Ca and S when compared to bed materials (Table S2), consistent with carbonate weathering and sulfide oxidation of the sedimentary rocks (Calmels et al., 2011). The coupled loss of Re and OC_{petro} relative to an immobile element is evident in Taiwanese soils (Fig. 3). The results are consistent with observations from soil profiles elsewhere, where rocks had higher

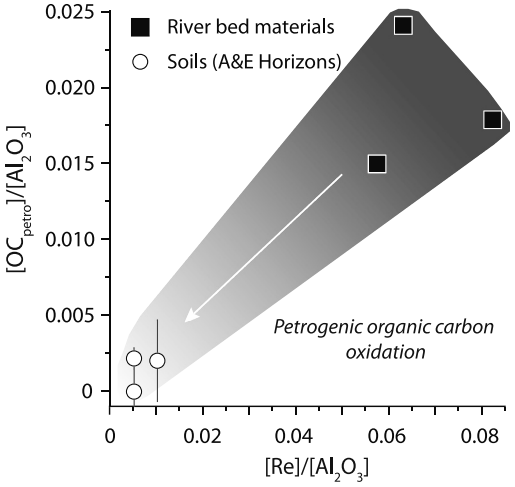

Fig. 3. Solid phase samples, river bed materials (black squares) and homogenized surface (A and E) soil horizons (white circles) from Taiwan. Rhenium concentration, [Re], and petrogenic organic carbon concentration, [OC_{petro}], have been normalized to an immobile element (aluminum, Al_2O_3) to track weathering processes. Arrow indicates coupled loss of Re and OC_{petro} from soil horizons from Taiwan confirming work on OC_{petro}-rich lithologies elsewhere (Jaffe et al., 2002). Vertical lines show propagated uncertainty on [OC_{petro}] (Appendix A) if larger than the point size.

[OC_{petro}], higher [Re] and a lower metamorphic grade than Taiwan (Jaffe et al., 2002).

4. Discussion

4.1. Insights on the source of dissolved rhenium

The association of Re and OC_{petro} in sedimentary rocks and the solubility of Re upon oxidation has lead previous work to suggest that $[Re]_{diss}$ may provide a robust tracer of OC_{petro} oxidation reactions (e.g. Dalai et al., 2002). However, it is important to assess the source of $[Re]_{diss}$ and address the validity of assumptions which link dissolved Re flux to OC_{petro} oxidation. First, the solid residue of chemical weathering provides insight on Re mobilization to the dissolved load. Bulk soil samples from Taiwan have lower [OC_{petro}] and [Re] when compared to the river bed materials (Fig. 3), which are likely to have a composition close to unweathered bedrock following their recent mobilization by bedrock landslides (Hovius et al., 2000). This result is consistent with observations of coupled Re and OC_{petro} loss made on soil profiles elsewhere (Peucker-Ehrenbrink and Hannigan, 2000; Jaffe et al., 2002) and suggests coupled oxidative weathering of Re and OC_{petro}. Once oxidized to the perrhenate anion ReO_4^-, Re is soluble in oxygenated waters (Eh > 0 V) with pH ranges 5.5–9.5 (Brookins, 1986). As a result, Re loss from soils should be recorded in the $[Re]_{diss}$ of rivers and its concentration influenced by the rate of weathering of the Re-bearing substrate (Colodner et al., 1993).

In river waters, previous work has suggested that a correlation between $[Re]_{diss}$ and $[SO_4]$ may imply a common source (i.e. sulfide minerals) during weathering (Miller et al., 2011). In Taiwan, sulfide oxidation is an important weathering reaction and the dominant source of SO_4^{2-} to rivers (Yoshimura et al., 2001; Calmels et al., 2011) and so the weak correlation between $[SO_4]$ and $[Re]_{diss}$ in Taiwan (Fig. 1A) may suggest sulfide minerals are not the dominant host of Re (Selby and Creaser, 2003). While this is consistent with the available measurements from soils and river bed materials in Taiwan (Fig. 3), it contrasts with previous conclusions drawn from observations linking $[Re]_{diss}$ to $[SO_4]$ in Himalayan rivers (Dalai et al., 2002) and globally (Miller et al., 2011). The discrepancy can be reconciled by noting that while the global trend between $[Re]_{diss}$ and $[SO_4]$ is significant ($r = 0.44$; $P < 0.0001$), it is extremely scattered (Fig. 1A). For $[Re]_{diss}$ values similar to Taiwan, the global data shows $[Re]_{diss}$ varies by >50 pmol L^{-1} for a given $[SO_4]$. Therefore, we propose that the global correlation does not indicate a common source of Re and SO_4^{2-}, but instead reflects changes in evaporation and/or dilution which set a first order control on all dissolved ion concentrations, especially in large rivers (Gaillardet et al., 1999). This would also explain why $[Re]_{diss}$ is better correlated with [Ca] ($r = 0.57$; $P < 0.0001$) in the same compilation of data shown in Fig. 1A. We are therefore wary of using correlations between dissolved ion concentrations to interpret a common source during chemical weathering (cf. Miller et al., 2011).

The significant correlation between $[Re]_{diss}$ in Taiwan rivers and the catchment-average suspended sediment concentration between 1970 and 1999 (Fig. 2) suggests that the rate of physical erosion over recent decades plays a major role in controlling $[Re]_{diss}$ of a catchment. This observation sheds new light on the weathering processes which mobilize Re from rocks to the dissolved phase. Physical erosion in Taiwan is dominated by bedrock landslides which scour deep (>1 m) into the rock mass (Hovius et al., 2000). An increase in the decadal average erosion rate therefore reflects an increase in the frequency at which unweathered bedrock is exposed at the surface by landslides. If weathering reactions are mainly limited by the supply of new minerals, then increased physical erosion rate should result in an increase in the concentration of dissolved products in river waters. Previous work has hypothesized that OC_{petro} oxidation in soils under present atmospheric O_2 levels are limited by the supply of OC_{petro} to an oxidative weathering zone near the surface (Petsch et al., 2000; Bolton et al., 2006) and may be enhanced by microbial assimilation in surface soils (Petsch et al., 2001). Therefore, the observed increase in $[Re]_{diss}$ with erosion rate (Fig. 2) support this hypothesis and suggest that supply limits OC_{petro} oxidative weathering, even at the very high rates of physical erosion in Taiwan.

The decoupling between $[Re]_{diss}$ and major elements with increasing runoff, such as [Na] (Figs. 1B and C), is also consistent with this explanation and suggests Re is mobilized from surface soils. Having taken rainwater inputs into account, dissolved Na (and Mg, Ca) is predominantly sourced from the inorganic rock matrix by acid hydrolysis reactions (Gaillardet et al., 1999; Tipper et al., 2006; Calmels et al., 2011). Laboratory experiments on fresh minerals show that acid hydrolysis reactions occur <10 times slower than oxidation weathering reactions (Chang and Berner, 1999; White and Brantley, 2003). Therefore longer flow paths which lengthen the timescales of fluid–rock interaction are required to elevate [Na] (Maher et al., 2011) and so [Na] is strongly diluted with increasing runoff (Fig. 1C). As a result, groundwater inputs which are most significant at low runoff can make up a large proportion (~70%) of the Na flux in Taiwan (Calmels et al., 2011). In contrast, Re is not diluted with runoff (Fig. 1B) and so groundwater inputs are likely to be relatively minor. Overall, the behavior of $[Re]_{diss}$ (Figs. 1B and 2) is more consistent with it being liberated from an oxygenated surface weathering zone by oxidation reactions which occur much quicker than acid hydrolysis.

The observation that oxidative weathering of OC_{petro} is supply-limited may seem at odds with measurements of significant export of unweathered OC_{petro} in the suspended load of Taiwanese rivers (Hilton et al., 2010, 2011). However, this reflects the dominant role of bedrock landslides in the erosion of mountain belts like Taiwan (Hovius et al., 2000). Landslides erode the weathering products from thin soils, which can be fully depleted in OC_{petro} (Fig. 3) and delivered them to river channels. However, the volume of bedrock landslides increases as a power law (exponent > 1.2) of the landslide area (Larsen et al., 2010) and so large, deep-seated landslides can deliver significant amounts of unweathered OC_{petro} to channels (Hilton et al., 2008b), overwhelming soil inputs. Thus a large

Table 1
Rhenium-derived OC_{petro} oxidation rate estimates for river catchments in Taiwan.

Catchment	Drainage area (km^2)	Suspended sediment yield ($t\,km^{-2}\,yr^{-1}$)[a]	Water discharge ($g\,yr^{-1}$)[a]	Decadal average SSC ($g\,L^{-1}$)[a]	n[b]	$[Re]_{diss}$ ($pmol\,L^{-1}$)	RSD[c] (%)	Re flux ($g\,yr^{-1}$)	OC_{petro} oxidation rate ($tC\,km^{-2}\,yr^{-1}$)[d]
Wulu	639	17 371	1.41E+15	7.9	3	14	10	3629	12–22
Yenping	476	19 118	1.00E+15	9.1	1	13	–	2417	11–19
Hsiukuluan	249	12 851	6.23E+14	5.1	1	10	–	1192	10–18
Hualien	1506	20 850	3.16E+15	9.9	2	20	21	11 634	17–30
Liwu	435	33 103	1.04E+15	13.8	6	21	22	4010	20–35
Chenyoulan	367	8719	6.97E+14	4.6	3	9	2	1130	7–12
Upper Chenyoulan	205	2927	4.10E+14	1.5	1	5	–	358	4–7
Laonung	853	10 785	1.62E+15	5.7	1	5	–	1505	4–7
Taimarli	190	2105	4.37E+14	0.9	1	6	–	458	5–9
Chihpen	166	21 687	3.98E+14	9.0	1	8	–	571	7–13
Taiwan average	35 980	10 672	4.98E+16	–	10	13	53	122 308	7–13

[a] Averages from 1970 to 1999 (Dadson et al., 2003), with suspended sediment concentration (SSC) calculated from decadal mean sediment transfer and water discharge.
[b] Number of $[Re]_{diss}$ analyses per catchment.
[c] Relative Standard Deviation (RSD) on $[Re]_{diss}$ measurements.
[d] Range of estimates derived from the range of measured [Re]:[OC_{petro}] ratios in river bed materials (Table S2).

proportion of the exhumed OC_{petro} does not spend significant time in the weathering zone before being exported by rivers. Bedrock landslides can therefore explain both the high rates of OC_{petro} oxidation by increasing mineral supply at landslide sites (Fig. 2) and also the rapid fluvial export and re-burial of un-weathered OC_{petro} offshore Taiwan (Kao et al., 2014).

4.2. Dissolved rhenium flux and estimates of OC_{petro} oxidation

The observed link between $[Re]_{diss}$ and sediment yield (Fig. 2), along with the coupled loss of Re and OC_{petro} from soils in Taiwan (Fig. 3), suggest that $[Re]_{diss}$ provides a powerful proxy of OC_{petro} oxidation in Taiwan. Here we describe how the dissolved Re flux can provide insight on the CO_2 release by OC_{petro} oxidation, and consider the assumptions which need to be applied. The first step is to quantify the dissolved Re flux, accounting for systematic changes in concentration with runoff (Calmels et al., 2011). $[Re]_{diss}$ was not diluted with increasing runoff (Fig. 1B) and so Re flux can be quantified robustly using an average $[Re]_{diss}$. Re fluxes for individual catchments were calculated, based on between 1 and 6 samples per catchment (Table 1). While this is relatively small number of samples and catchment-scale Re flux may be refined by longer records, the number is similar to work quantifying Re fluxes in large rivers (Miller et al., 2011). At the mountain belt scale, the area-weighted mean $[Re]_{diss}$ in the sampled catchments is 13.2 ± 3.7 $pmol\,L^{-1}$ ($n = 10$, ± 2 SE, Table 1) and for an annual water discharge of 49.8 $km^3\,yr^{-1}$ (Dadson et al., 2003) the dissolved Re flux from Taiwan to the ocean is 700 ± 200 $mol\,yr^{-1}$. The Re yield estimates from individual river catchments in Taiwan were correlated to the sediment yield measured independently from 1970 to 1999 (Fig. 4A).

Having quantified the oxidized Re flux from river catchments, the OC_{petro} oxidation rate can be estimated provided that the initial [Re]:[OC_{petro}] of rocks is known. In addition, two assumptions are necessary: i) that Re is hosted primarily in OC_{petro}; and ii) that oxidation mobilizes $[Re]_{diss}$ and releases CO_2 from OC_{petro} at the same rate. The first assumption would appear to be valid based on the high Re contents of organic matter isolated from sedimentary rocks, with OC_{petro} shown to dominate the total mass of Re (Cohen et al., 1999; Pierson-Wickmann et al., 2002; Selby and Creaser, 2003; Rooney et al., 2012). However, some Re can be sourced from inorganic phases (Dalai et al., 2002), which may host ~30% of Re in marine sediments (Selby and Creaser, 2003). A Re-derived OC_{petro} oxidation rate will be an overestimation if this is the case. Regarding the second assumption, weathering products from soil horizons in Taiwan show coupled loss of OC_{petro} and Re during weathering (Fig. 3). However, soil profiles from elsewhere have shown that oxidation can result in slightly higher losses of Re from the solid phase (~99%) compared to losses of OC_{petro} (~80%) (Jaffe et al., 2002; Pierson-Wickmann et al., 2002). In addition, rocks in Taiwan can contain graphitic-OC_{petro} (Beyssac et al., 2007) which has been shown to be resilient to chemical and physical breakdown in river catchments (Galy et al., 2008a; Bouchez et al., 2010) but it is not known whether graphitic-OC_{petro} contains Re. Based on our current understanding of Re mobility, these assumptions mean that the dissolved Re flux is likely to represent an upper bound on the OC_{petro} oxidation rate. These details warrant future research to refine the Re-proxy, however our new findings on the mobility of Re during weathering in Taiwan (Figs. 2 and 3) suggest that a Re-derived estimate of OC_{petro} oxidation rate offers a robust, upper bound quantification.

To calculate OC_{petro} oxidation rates, the dissolved Re flux (Fig. 4A) must be combined with measurements of the initial [Re] to [OC_{petro}] ratio of sedimentary rocks in the catchment. Individual bedrock samples may significantly overestimate the heterogeneity present at the catchment scale and instead, river bed materials can provide a robust average sample of the major geological formations upstream (Galy et al., 2008a; Hilton et al., 2010). In Taiwan, [Re]:[OC_{petro}] of the three river bed material samples ranged within a factor of two, from 2.6×10^{-7} to 4.6×10^{-7}. While the sample set of river bed materials is small ($n = 3$), we note that the samples analyzed here have nitrogen to OC ratios between 0.1 and 0.2 (Table S2) which covers a range of compositions representative of OC_{petro} in the major geological formations (Hilton et al., 2010). The samples provide a plausible range of [Re]:[OC_{petro}] of the source and allow us to assess a range of CO_2 emission estimates. With the knowledge that OC_{petro} oxidation rates derived from dissolved Re flux are likely to be an upper bound, and that the initial [Re]:[OC_{petro}] of rocks is the main source of uncertainty, we estimate a maximum CO_2 release by OC_{petro} oxidation of between 0.27 and 0.47 $MtC\,yr^{-1}$ from this mountain belt. Normalized over the island source area (35 980 km^2) the CO_2 yield is 7.4–13.0 $tC\,km^{-2}\,yr^{-1}$. This is a significant carbon transfer and is higher than estimates of CO_2 drawdown by silicate weathering in mountain belts of 3–4 $tC\,km^{-2}\,yr^{-1}$ (Jacobson and Blum, 2003). The results suggest that in Taiwan the chemical denudation of OC_{petro} by oxidation represents <20% of the total OC_{petro} denudation (weathering plus erosion) with ~1.7 $MtC\,yr^{-1}$ exported to the ocean in solid form (Hilton et al., 2011). In contrast, the extensive floodplains downstream of the Himalaya and Andes mountains (of the Ganges and Amazon rivers, respectively) provide time for additional OC_{petro} oxidation, removing all but the most resilient OC_{petro}

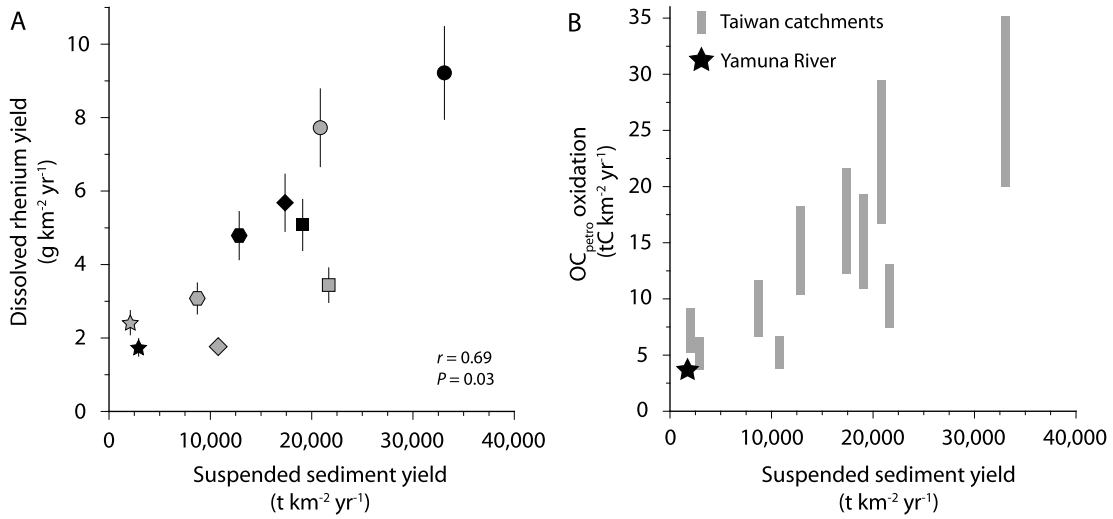

Fig. 4. A. Dissolved rhenium (Re) yield ($g\,km^{-2}\,yr^{-1}$) versus average suspended sediment yield 1970–1999 (Dadson et al., 2003) for individual catchments in Taiwan (symbols as in Fig. 2). Vertical bars denote the mean standard deviation in dissolved Re concentration in the sampled catchments (Table 1). **B.** Petrogenic organic carbon (OC_{petro}) oxidation rates ($tC\,km^{-2}\,yr^{-1}$) calculated using the dissolved Re yield for Taiwan catchments (gray rectangles) versus suspended sediment yield. The range of estimates represent uncertainty based on the measured range of Re to OC_{petro} ratios in river bed materials. The black star shows OC_{petro} oxidation rate estimated previously using dissolved Re flux from the Yamuna River catchment, Himalaya (Dalai et al., 2002).

(graphite) from the solid load (Galy et al., 2008a; Bouchez et al., 2010, 2014). In Taiwan, the combination of bedrock landslides (see Section 4.1), rapid fluvial transit times and strong land–ocean coupling mean that despite the rapid OC_{petro} oxidation rates (Fig. 4B) the majority of exhumed OC_{petro} (>80%) is eroded and reburied offshore Taiwan (Kao et al., 2014).

The Re-derived OC_{petro} oxidation rates for individual catchments (Table 1) are positively related to the decadal suspended sediment yield (Fig. 4B). The catchment-scale OC_{petro} oxidation rates may be refined using longer time-series of $[Re]_{diss}$ measurements and catchment-specific [Re]:[OC_{petro}] ratios of river bed materials. Nevertheless, the relationship is consistent with a Re-derived OC_{petro} oxidation rate made using the same methods in the Yamuna River draining the Himalaya (9600 km^2), where OC_{petro} oxidation is estimated to release ~4 $tC\,km^{-2}\,yr^{-1}$ of CO_2 (Dalai et al., 2002) with denudation ~1700 $t\,km^{-2}\,yr^{-1}$ (Lupker et al., 2012) (Fig. 4B). Our new data confirm the hypothesis that physical erosion rate is a major control on OC_{petro} oxidation and moderates CO_2 release during weathering (Petsch et al., 2000), even at the very high erosion rates experienced in Taiwan.

4.3. The net OC budget of a mountain belt

The Re-derived OC_{petro} oxidation rate can be used to assess the net OC budget of a mountain belt for the first time. Physical erosion in Taiwan results in the mobilization of $OC_{biosphere}$ from soils and vegetation and its transported to the oceans in river suspended load (Hilton et al., 2008a). The erosion of the $OC_{biosphere}$ results in the export of ~0.5 $MtC\,yr^{-1}$ (10^{12} $gC\,yr^{-1}$) of $OC_{biosphere}$ from Taiwan, a value which is thought to be conservative (Hilton et al., 2012). Recent observations show that $OC_{biosphere}$ is efficiently preserved (70–100%) in sediments offshore Taiwan (Kao et al., 2014), in analogy with tectonic margins elsewhere (Galy et al., 2007; Blair and Aller, 2012), with an estimate of CO_2 sequestration of 0.5–0.6 $MtC\,yr^{-1}$ by terrestrial $OC_{biosphere}$ burial (Kao et al., 2014). Additional OC burial occurs as marine organic matter and has not been quantified. Therefore, given that the estimate of CO_2 release provided here is likely to be an upper bound (Section 4.2), and that the estimates of CO_2 drawdown are likely to be conservative (Kao et al., 2014), the assessment of net OC sequestration will also be conservative. Taking the estimated bounds into account, we find that cycling of OC during the erosion and weathering of Taiwan presently acts as a net sink of atmospheric CO_2 (Fig. 5).

The findings can be compared to the Ganges–Brahmaputra river system draining the Himalaya, where source to sink sediment and OC transfers have been partly quantified (France-Lanord and Derry, 1997; Galy et al., 2007, 2008a; Gaillardet and Galy, 2008). There terrestrial $OC_{biosphere}$ is buried efficiently in rapidly accumulating, O_2 depleted waters of the Bay of Bengal and sequesters 3.7 $MtC\,yr^{-1}$ derived from a continental source area of ~1.6×10^6 km^2 (Galy et al., 2007). In contrast, ~0.8 $MtC\,yr^{-1}$ of OC_{petro} is thought to be oxidized during floodplain transport once OC_{petro} has left the mountain belt (Galy et al., 2008a). OC_{petro} oxidation rates have not been quantified in Himalayan catchments where CO_2 emissions may be higher due to faster physical erosion (e.g. Fig. 4B). However, denudation rates in the Himalaya are lower than Taiwan (Dadson et al., 2003; Lupker et al., 2012), and the upward corrected OC_{petro} oxidation rate is unlikely to counter the CO_2 sink by burial of $OC_{biosphere}$.

Together with our new data, these findings suggest that in mountain belts located in the subtropics, the CO_2 sequestration achieved by $OC_{biosphere}$ export and burial is greater than the CO_2 emissions by geological respiration during oxidative weathering of OC_{petro} (Fig. 5). The frontal Himalaya and Taiwan experience high physical erosion rates driven by fluvial incision and bedrock landsliding, which can supply abundant OC_{petro} for oxidation (Hilton et al., 2011). However, both orogenic belts feature productive terrestrial biomass which is eroded rapidly and is buried with clastic sediment (Galy et al., 2007; Hilton et al., 2012; Kao et al., 2014). The balance of these OC fluxes presently act as a sink of CO_2 (Fig. 5). However, the net OC cycle in Taiwan appears to be sensitive to small increases in the CO_2 release by OC_{petro} weathering, which will vary spatially (and temporally) in response to changes in the rate of physical erosion (Fig. 4B). It is also sensitive to changes in the distribution of mountain forest and soil which might reduce the CO_2 sequestration associated with erosion and burial of $OC_{biosphere}$ (Hilton et al., 2012). These factors should be central in controlling the impact of mountain building on the long-term sequestration of CO_2 in the lithosphere (Derry and France-Lanord, 1996) and the influence of orogenesis on the evolution of atmospheric CO_2 and O_2 concentrations (Caldeira et al., 1993; Berner and Canfield, 1989; Gaillardet and Galy, 2008). The im-

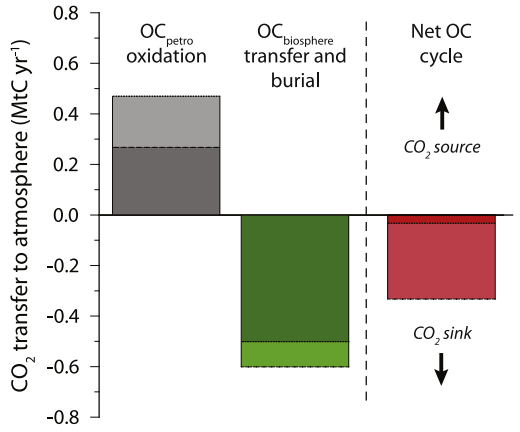

Fig. 5. Net organic carbon balance in Taiwan expressed in terms of CO_2 fluxes to (positive) and from (negative) the atmosphere. Petrogenic organic carbon (OC_{petro}) oxidation rate derived from dissolved Re flux (Fig. 4A, this study) is differenced from the transfer and burial of OC from the terrestrial biosphere ($OC_{biosphere}$) transfer and burial (Hilton et al., 2012; Kao et al., 2014) to assess the net OC cycle, with upper (dashed) and lower (dotted) bounds for net CO_2 sequestration.

pact of changing physical erosion rates on the global carbon cycle has received renewed attention via the process of sulfide oxidative coupled to carbonate weathering (Calmels et al., 2007) over interglacial–glacial cycles (Georg et al., 2013) and during the Cenozoic (Torres et al., 2014). Our findings suggest a more direct link via the oxidative weathering of OC_{petro} and CO_2 release (Fig. 4B) and better understanding the rates and patterns of OC_{petro} oxidation remains a research priority.

5. Conclusions

The rates and controls on CO_2 release by OC_{petro} oxidation in a mountain belt were assessed using the trace element Re. In solid weathering products from Taiwan, Re loss was coupled to OC_{petro} loss (Fig. 3), confirming previous work from soil profiles on OC_{petro}-rich rocks. In river waters from Taiwan, $[Re]_{diss}$ was positively, significantly correlated with the decadal average suspended sediment concentration (1970–1999), a measure of physical erosion rate normalized by runoff (Fig. 2). We estimate Re flux for the sampled catchments and find that the Re yield also increases with sediment yield (Fig. 4A). An increase in $[Re]_{diss}$ and Re flux in basins which erode more rapidly is consistent with the dominant source of Re from a surficial weathering zone, where oxidation reactions are limited by mineral supply.

The Re flux measurements are used to estimate the CO_2 release by OC_{petro} oxidation with knowledge of the initial [Re]:[OC_{petro}] of bedrocks, and assuming: i) that Re is hosted primarily in OC_{petro}; and ii) congruent release of $[Re]_{diss}$ and CO_2 from OC_{petro} occurs during oxidative weathering. We note that the first assumption is validated by previous work, but may lead to an overestimation of CO_2 flux if some dissolved Re is derived from inorganic minerals. The second assumption appears to be valid based on our measurements of OC_{petro} and Re loss in weathering products in Taiwan (Fig. 3) and is supported by previous observations of coupled loss of Re and OC_{petro} in soil weathering profiles. However, based on our current understanding of Re mobility, it may lead to an overestimation of OC_{petro} oxidation rate if Re is liberated more rapidly during weathering. The patterns of CO_2 release across Taiwan are controlled by physical erosion rate (Fig. 4B), confirming mountain belts as hotspots of CO_2 release by geological respiration. The absolute rates of CO_2 emission in river catchments estimated from dissolved Re flux are likely to be an upper bound. Nevertheless, at the mountain belt scale, the OC_{petro} oxidation rate is not sufficient to negate the estimated CO_2 drawdown by erosion of OC from the terrestrial biosphere, its fluvial transport and marine burial offshore. Mountain building in Taiwan presently acts as an OC sink, sequestering atmospheric CO_2 during weathering and erosion.

Acknowledgements

Data associated with this research can be found in the supplementary materials. The research was funded by a Natural Environment Research Council (NERC), UK, New Investigator Grant to R.G. Hilton (NE/I001719/1) and by a CNRS EC2CO grant ('OXYMORE') to J. Gaillardet. R.G. Hilton acknowledges Research Leave from Durham University and funding from IPG, Paris, as a Visiting Professor. We thank F. Campas and J. Moureau for laboratory and analytical assistance and A. Galy, A.J. West, E. Tipper, D. Selby and J. Bouchez for discussions, and L. Derry and three anonymous referees for their comments which improved this work.

Appendix A. Quantification of OC_{petro} content in soil samples

The OC_{petro} content (%) of soil samples was determined using F_{mod} measurements (Hilton et al., 2013) and a binary mixing model which assumes contemporary inputs ($OC_{biosphere}$) mix with radiocarbon depleted OC_{petro} (e.g. Galy et al., 2008a; Hilton et al., 2008a; Clark et al., 2013):

$$(F_{mod})_{petro} \times f_{petro} + (F_{mod})_{biosphere} \times f_{biosphere} = (F_{mod})_{sample} \quad (A.1)$$

where f denotes the fraction of OC derived from petrogenic and biosphere sources (f_{petro} and $f_{biosphere}$, respectively) where $f_{petro} + f_{biosphere} = 1$ for a binary mixture. The radiocarbon activity of petrogenic OC $(F_{mod})_{petro} = 0$ by definition (radiocarbon content indistinguishable from background). The C-weighted mean F_{mod} of upper soil horizons in Taiwan has been measured by Hilton et al. (2008a, 2008b) as $F_{mod} = 0.98 \pm 0.07$ ($n = 10$, $\pm$SD) and this is taken as the radiocarbon activity of the $OC_{biosphere}$ end member composition $(F_{mod})_{biosphere}$.

Eq. (A.1) can be solved for f_{petro} and the measured f_{petro} combined with measured total organic carbon concentration (C_{org}, %) to quantity the [OC_{petro}], in % (Kao et al., 2014). The uncertainty on [OC_{petro}] content of soils is derived from the propagation of the variability on the end member compositions (Fig. 3). The analysis provides an upper estimate of OC_{petro} content because aging of soil organic matter can also deplete ^{14}C content, rather than OC_{petro} addition (Hilton et al., 2013). Previous work has established that OC in the river bed material samples is dominated by OC_{petro} using element ratios and stable carbon isotopes (Hilton et al., 2010).

Appendix B. Supplementary material

Supplementary material related to this article can be found online at http://dx.doi.org/10.1016/j.epsl.2014.06.021.

References

Anbar, A.D., Creasar, R.A., Papanastassiou, D.A., Wasserburg, G.J., 1992. Rhenium in seawater: confirmation of generally conservative behaviour. Geochim. Cosmochim. Acta 56, 4099–4103.

Berner, R.A., Canfield, D.E., 1989. A new model for atmospheric oxygen over Phanerozoic time. Am. J. Sci. 289, 333–361.

Beyssac, O., et al., 2007. Late Cenozoic metamorphic evolution and exhumation of Taiwan. Tectonics 26, TC6001. http://dx.doi.org/10.1029/2006TC002064.

Birck, J.L., Barman, M.R., Capmas, F., 1997. Re–Os isotopic measurements at the femtomole level in natural samples. J. Geostand. Geoanal. 20, 19–27.

Blair, N.E., Aller, R.C., 2012. The fate of terrestrial organic carbon in the marine environment. Annu. Rev. Mar. Sci. 4, 17.1–17.23.

Bolton, E.W., Berner, R.A., Petsch, S.T., 2006. The weathering of sedimentary organic matter as a control on atmospheric O_2: II. Theoretical modeling. Am. J. Sci. 306, 575–615.

Bouchez, J., et al., 2010. Oxidation of petrogenic organic carbon in the Amazon floodplain as a source of atmospheric CO_2. Geology 38, 255–258.

Bouchez, J., Gaillardet, J., France-Lanord, C., Maurice, L., Dutra-Maia, P., 2011. Grain-size controls of river suspended sediment geochemistry: insights from Amazon River depth profiles. Geochem. Geophys. Geosyst. 12, GC00380.

Bouchez, J., et al., 2014. Source, transport and fluxes of Amazon River particulate organic carbon: insights from river sediment depth-profiles. Geochim. Cosmochim. Acta 133, 280–298.

Brookins, D.G., 1986. Rhenium as an analog for fissiogenic technetium: Eh–pH diagram (25 °C, 1 bar) constraints. Appl. Geochem. 1, 513–517.

Caldeira, K., Arthur, M.A., Berner, R.A., Lasaga, A.C., 1993. Cooling in the late Cenozoic. Nature 361, 123–124.

Calmels, D., Gaillardet, J., Brenot, A., France-Lanord, C., 2007. Sustained sulfide oxidation by physical erosion processes in the Mackenzie River basin: climatic perspectives. Geology 35, 1003–1006.

Calmels, D., et al., 2011. Contribution of deep groundwater to the weathering budget in a rapidly eroding mountain belt, Taiwan. Earth Planet. Sci. Lett. 303, 48–59.

Chang, S., Berner, R.A., 1999. Coal weathering and the geochemical carbon cycle. Geochim. Cosmochim. Acta 63, 3301–3310.

Clark, K.C., et al., 2013. New views on "old" carbon in the Amazon river: insight from the source of organic carbon eroded from the Peruvian Andes. Geochem. Geophys. Geosyst. 14, 1644–1659. http://dx.doi.org/10.1002/ggge.20122.

Cohen, A.S., Coe, A.L., Bartlett, J.M., Hawkesworth, C.J., 1999. Precise Re–Os ages of organic-rich mudrocks and the Os isotope composition of Jurassic seawater. Earth Planet. Sci. Lett. 167, 159–173.

Colodner, D., et al., 1993. The geochemical cycles of rhenium: a reconnaissance. Earth Planet. Sci. Lett. 117, 205–221.

Crusius, J., Thomson, J., 2000. Comparative behavior of authigenic Re, U, and Mo during reoxidation and subsequent long-term burial in marine sediments. Geochim. Cosmochim. Acta 64, 2233–2242.

Crusius, J., Calvert, S.E., Pedersen, T.F., Sage, D., 1996. Rhenium and molybdenum enrichments in sediments as indicators of oxic, suboxic and anoxic conditions of deposition. Earth Planet. Sci. Lett. 145, 65–79.

Cumming, V.M., Selby, D., Lillis, P.G., Lewan, M.D., 2014. Re–Os geochronology and Os isotope fingerprinting of petroleum sourced from a Type I lacustrine kerogen: insights from the natural Green River petroleum system in the Uinta Basin and hydrous pyrolysis experiments. Geochim. Cosmochim. Acta 138, 32–56.

Dadson, S.J., et al., 2003. Links between erosion, runoff variability and seismicity in the Taiwan orogen. Nature 426, 648–651.

Dalai, T.K., Singh, S.K., Trivedi, J.R., Krishnaswami, S., 2002. Dissolved rhenium in the Yamuna River System and the Ganga in the Himalaya: role of black shale weathering on the budgets of Re, Os, and U in rivers and CO_2 in the atmosphere. Geochim. Cosmochim. Acta 66, 29–43.

Derry, L.A., France-Lanord, C., 1996. Neogene growth of the sedimentary organic carbon reservoir. Paleoceanography 11, 267–275.

France-Lanord, C., Derry, L.A., 1997. Organic carbon burial forcing of the carbon cycle from the Himalayan erosion. Nature 390, 65–67.

Gaillardet, J., Galy, A., 2008. Himalaya – carbon sink or source? Science 320, 1727–1728.

Gaillardet, J.B., Dupré, B., Louvat, P., Allègre, C.J., 1999. Global silicate weathering and CO_2 consumption rates deduced from the chemistry of large rivers. Chem. Geol. 159, 3–30.

Galy, V., et al., 2007. Efficient organic carbon burial in the Bengal fan sustained by the Himalayan erosional system. Nature 450, 407–410.

Galy, V., Beyssac, O., France-Lanord, C., Eglinton, T.I., 2008a. Recycling of graphite during Himalayan erosion: a geological stabilization of carbon in the crust. Science 322, 943–945.

Galy, V., France-Lanord, C., Lartiges, B., 2008b. Loading and fate of particulate organic carbon from the Himalaya to the Ganga–Brahmaputra delta. Geochim. Cosmochim. Acta 72, 1767–1787.

Georg, R.B., West, A.J., Vance, D., Newmand, K., Halliday, A.N., 2013. Is the marine osmium isotope record a probe for CO_2 release from sedimentary rocks? Earth Planet. Sci. Lett. 367, 28–38.

Hayes, J.M., Waldbauer, J.R., 2006. The carbon cycle and associated redox processes through time. Philos. Trans. R. Soc. Lond. B 361, 931–950.

Hayes, J.M., Strauss, H., Kaufman, A.J., 1999. The abundance of ^{13}C in marine organic matter and isotopic fractionation in the global biogeochemical cycle of carbon during the past 800 Ma. Chem. Geol. 161, 103–125.

Hilton, R.G., et al., 2008a. Tropical-cyclone-driven erosion of the terrestrial biosphere from mountains. Nat. Geosci. 1, 759–762.

Hilton, R.G., Galy, A., Hovius, N., 2008b. Riverine particulate organic carbon from an active mountain belt: importance of landslides. Glob. Biogeochem. Cycles 22, GB1017. http://dx.doi.org/10.1029/2006GB002905.

Hilton, R.G., Galy, A., Hovius, N., Horng, M.-J., Chen, H., 2010. The isotopic composition of particulate organic carbon in mountain rivers of Taiwan. Geochim. Cosmochim. Acta 74, 3164–3181.

Hilton, R.G., Galy, A., Hovius, N., Horng, M.-J., Chen, H., 2011. Efficient transport of fossil organic carbon to the ocean by steep mountain rivers: an orogenic carbon sequestration mechanism. Geology 39, 71–74.

Hilton, R.G., et al., 2012. Climatic and geomorphic controls on the erosion of terrestrial biomass from subtropical mountain forest. Glob. Biogeochem. Cycles 26, GB3014.

Hilton, R.G., Galy, A., West, A.J., Hovius, N., Roberts, G.G., 2013. Geomorphic control on the $\delta^{15}N$ of mountain forests. Biogeosciences 10, 1693–1705.

Hovius, N., Stark, C.P., Chu, H.-T., Lin, J.-C., 2000. Supply and removal of sediment in a landslide-dominated mountain belt: Central Range, Taiwan. J. Geol. 108, 73–89.

Huffman, E.H., Oswalt, R.L., Williams, L.A., 1956. Anion-exchange separation of molybdenum and technetium and of tungsten and rhenium. J. Inorg. Nucl. Chem. 3, 49–53.

Jacobson, A.D., Blum, J.D., 2003. Relationship between mechanical erosion and atmospheric CO_2 consumption in the New Zealand Southern Alps. Geology 31, 865–868.

Jaffe, L.A., Peucker-Ehrenbrink, B., Petsch, S.T., 2002. Mobility of rhenium, platinum group elements and organic carbon during black shale weathering. Earth Planet. Sci. Lett. 198, 339–353.

Kao, S.J., et al., 2014. Preservation of terrestrial organic carbon in marine sediments offshore Taiwan: mountain building and atmospheric carbon dioxide sequestration. Earth Surf. Dyn. 2, 127–139.

Keller, C.K., Bacon, D.H., 1998. Soil respiration and georespiration distinguished by transport analyses of vadose CO_2, $^{13}CO_2$ and $^{14}CO_2$. Glob. Biogeochem. Cycles 12, 361–372.

Larsen, I.J., Montgomery, D.R., Korup, O., 2010. Landslide erosion controlled by hillslope material. Nat. Geosci. 3, 247–251. http://dx.doi.org/10.1038/ngeo776.

Lupker, M., et al., 2012. ^{10}Be-derived Himalayan denudation rates and sediment budgets in the Ganga basin. Earth Planet. Sci. Lett. 333–334, 146–156.

Maher, K., 2011. The role of fluid residence time and topographic scales in determining chemical fluxes from landscapes. Earth Planet. Sci. Lett. 312, 48–58.

McKay, J.L., Pedersen, T.F., Mucci, A., 2007. Sedimentary redox conditions in continental margin sediments (N.E. Pacific) – influence on the accumulation of redox-sensitive trace metals. Chem. Geol. 238, 180–196.

Meybeck, M., 1987. Global chemical weathering of surficial rocks estimated from river dissolved loads. Am. J. Sci. 287, 401–428.

Miller, C.A., Peucker-Ehrenbrink, B., Walker, B.D., Marcantonio, F., 2011. Re-assessing the surface cycling of molybdenum and rhenium. Geochim. Cosmochim. Acta 75, 7146–7179.

Petsch, S.T., Berner, R.A., Eglinton, T.I., 2000. A field study of the chemical weathering of ancient sedimentary organic matter. Org. Geochem. 31, 475–487.

Petsch, S.T., Eglinton, T.I., Edwards, K.J., 2001. ^{14}C-dead living biomass: evidence for microbial assimilation of ancient organic matter during shale weathering. Science 292, 1127–1131.

Peucker-Ehrenbrink, B., Hannigan, R.E., 2000. Effects of black shale weathering on the mobility of rhenium and platinum group elements. Geology 28, 475–478.

Pierson-Wickmann, A.C., Reisberg, L., France-Lanord, C., 2002. Behavior of Re and Os during low-temperature alteration: results from Himalayan soils and altered black shales. Geochim. Cosmochim. Acta 66, 1539–1548.

Rahaman, W., Singh, S.K., Shukla, A.D., 2012. Rhenium in Indian rivers: sources, fluxes, and contribution to oceanic budget. Geochem. Geophys. Geosyst. 13, Q08019.

Ravizza, G.E., Turekian, K.K., Hay, B.J., 1991. The geochemistry of rhenium and osmium in recent sediments from the Black Sea. Geochim. Cosmochim. Acta 55, 3741–3752.

Rooney, A.D., Selby, D., Lewan, M.D., Lillis, P.G., Houzay, J.P., 2012. Evaluating Re–Os systematics in organic-rich sedimentary rocks in response to petroleum generation using hydrous pyrolysis experiments. Geochim. Cosmochim. Acta 77, 275–291.

Selby, D., Creaser, R.A., 2003. Re–Os geochronology of organic rich sediments: an evaluation of organic matter analysis methods. Chem. Geol. 200, 225–240.

Selvaraj, K., Chen, C.T.A., 2006. Moderate chemical weathering of subtropical Taiwan: constraints from solid-phase geochemistry of sediments and sedimentary rocks. J. Geol. 114, 101–116.

Stallard, R.F., 1998. Terrestrial sedimentation and the carbon cycle: coupling weathering and erosion to carbon burial. Glob. Biogeochem. Cycles 12, 231–257.

Stuiver, M., Polach, H.A., 1977. Discussion: reporting of ^{14}C data. Radiocarbon 19 (3), 355–363.

Sundquist, E.T., Visser, K., 2005. In: Schlesinger, W. (Ed.), Biogeochemistry. Elsevier, Oxford, pp. 425–472.

Tipper, E.T., et al., 2006. The short term climatic sensitivity of carbonate and silicate weathering fluxes: insight from seasonal variations in river chemistry. Geochim. Cosmochim. Acta 70, 2737–2754.

Torres, M.A., West, A.J., Li, G., 2014. Sulphide oxidation and carbonate dissolution as a source of CO_2 over geological timescales. Nature 507, 346–349.
Tsai, C.C., Chen, Z.S., Duh, C.T., Horng, F.W., 2001. Prediction of soil depth using a soil–landscape regression model: a case study on forest soils in southern Taiwan. Proc. Natl. Sci. Counc., Repub. China, Part B 26, 34–39.
Turowski, J.M., Hovius, N., Hsieh, M.L., Lague, D., Chen, M.C., 2008. Distribution of erosion across bedrock channels. Earth Surf. Process. Landf. 33, 353–363.
West, A.J., Galy, A., Bickle, M., 2005. Tectonic and climatic controls on silicate weathering. Earth Planet. Sci. Lett. 235, 211–228.
White, A.F., Brantley, S.L., 2003. The effect of time on the weathering of silicate minerals: why do weathering rates differ in the laboratory and the field? Chem. Geol. 202, 479–506.
Yoshimura, K., et al., 2001. Geochemical and stable isotope studies on natural water in the Taroko Gorge karst area, Taiwan – chemical weathering of carbonate rocks by deep source CO_2 and sulfuric acid. Chem. Geol. 177, 415–430.